



OPEN ACCESS

EDITED BY

Thomas R. Butts,
Purdue University, United States

REVIEWED BY

Parvathaneni Naga Srinivasu,
Prasad V. Potluri Siddhartha Institute of
Technology, India
Lakshmeeswari Gondi,
Gandhi Institute of Technology and
Management (GITAM), India

*CORRESPONDENCE

Canicius Mwitta

✉ cmwitta@uga.edu

Glen C. Rains

✉ grains@uga.edu

RECEIVED 19 February 2024

ACCEPTED 29 April 2024

PUBLISHED 16 May 2024

CITATION

Mwitta C, Rains GC and Prostko EP (2024)
Autonomous diode laser weeding mobile
robot in cotton field using deep learning,
visual servoing and finite state machine.
Front. Agron. 6:1388452.
doi: 10.3389/fagro.2024.1388452

COPYRIGHT

© 2024 Mwitta, Rains and Prostko. This is an
open-access article distributed under the terms
of the [Creative Commons Attribution License
\(CC BY\)](https://creativecommons.org/licenses/by/4.0/). The use, distribution or reproduction
in other forums is permitted, provided the
original author(s) and the copyright owner(s)
are credited and that the original publication
in this journal is cited, in accordance with
accepted academic practice. No use,
distribution or reproduction is permitted
which does not comply with these terms.

Autonomous diode laser weeding mobile robot in cotton field using deep learning, visual servoing and finite state machine

Canicius Mwitta^{1*}, Glen C. Rains^{2*} and Eric P. Prostko³

¹College of Engineering, University of Georgia, Athens, GA, United States, ²Department of Entomology, University of Georgia, Tifton, GA, United States, ³Department of Crop and Soil Sciences, University of Georgia, Tifton, GA, United States

Small autonomous robotic platforms can be utilized in agricultural environments to target weeds in their early stages of growth and eliminate them. Autonomous solutions reduce the need for labor, cut costs, and enhance productivity. To eliminate the need for chemicals in weeding, and other solutions that can interfere with the crop's growth, lasers have emerged as a viable alternative. Lasers can precisely target weed stems, effectively eliminating or stunting their growth. In this study an autonomous robot that employs a diode laser for weed elimination was developed and its performance in removing weeds in a cotton field was evaluated. The robot utilized a combination of visual servoing for motion control, the Robotic operating system (ROS) finite state machine implementation (SMACH) to manage its states, actions, and transitions. Furthermore, the robot utilized deep learning for weed detection, as well as navigation when combined with GPS and dynamic window approach path planning algorithm. Employing its 2D cartesian arm, the robot positioned the laser diode attached to a rotating pan-and-tilt mechanism for precise weed targeting. In a cotton field, without weed tracking, the robot achieved an overall weed elimination rate of 47% in a single pass, with a 9.5 second cycle time per weed treatment when the laser diode was positioned parallel to the ground. When the diode was placed at a 10° downward angle from the horizontal axis, the robot achieved a 63% overall elimination rate on a single pass with 8 seconds cycle time per weed treatment. With the implementation of weed tracking using DeepSORT tracking algorithm, the robot achieved an overall weed elimination rate of 72.35% at 8 seconds cycle time per weed treatment. With a strong potential for generalizing to other crops, these results provide strong evidence of the feasibility of autonomous weed elimination using low-cost diode lasers and small robotic platforms.

KEYWORDS

non-chemical weeding, robotic weeding, precision agriculture, weed detection, autonomous navigation, weed stem laser targeting

1 Introduction

Weeds can have detrimental effects on crop yield, causing heavy economic losses (Pimentel et al., 2000; Oerke, 2006; Gharde et al., 2018), and in most cases, even higher losses than pathogens and invertebrate pests (Oerke, 2006; Radicetti and Mancinelli, 2021).

Chemical weeding, manual weeding, and mechanical weeding have been the common practices for weed control in agricultural fields (Chauvel et al., 2012). Chemical weeding has been the most effective and most used weed control method (Buhler et al., 2000; Gianessi and Reigner, 2007; Abbas et al., 2018). However, weeds have evolved resistance to many chemistries, posing a threat to productivity (Powles et al., 1996; Shaner, 2014). Moreover, there are concerns about the negative impacts of the chemicals on the environment (Colbach et al., 2010; Abbas et al., 2018). Mechanical weeding approaches are not very efficient and can interfere with crop activities, potentially causing crop injury (Fogelberg and Gustavsson, 1999; Abbas et al., 2018), while manual weeding can be time consuming and is associated with high labor costs (Schuster et al., 2007; Bastiaans et al., 2008; Young et al., 2014).

Weeding can be labor-intensive, necessitating the hiring and management of labor. As evidence shows, labor costs in agriculture are increasing rapidly due to labor shortages (Guthman, 2017; Richards, 2018; Zahniser et al., 2018). Without alternative methods that are less labor-reliant, the development of agriculture will fall short of demand. Thanks to technology, multiple potential solutions have been investigated and implemented including taking advantage of autonomous robots to deliver management tools. The affordability of artificial intelligence, computer processors and sensors has enabled the automation of various agricultural tasks, including weeding, planting, and harvesting (Oliveira et al., 2021).

Autonomous weeding in agricultural fields demands high precision in effectively identifying the weeds, navigating the robot, and removing the weeds. These tasks are made difficult by the outdoor nature of the agricultural environment, which is subject to constant changes in illumination, weather, uneven terrain, and occlusion. Various techniques have been employed in attempts to overcome these challenges. For example, McCool et al. (2018) implemented mechanical and spraying mechanisms in their autonomous weed management robot, Agbot II, and utilized color segmentation in their weed detection. Blasco et al. (2002) used machine vision algorithms to identify weeds and remove them with an electric discharge. Furthermore, Pérez-Ruiz et al. (2014) introduced an autonomous mechanical weeding robot to remove intra-row weeds using movable hoes, utilizing odometry data and pre-programmed crop planting pattern, while Florance Mary and Yogaraman (2021) drilled the weeds to the ground with their autonomous robot that utilized deep learning computer algorithms for weed detection. Despite their successful implementations, these studies focused on destructive mechanical solutions with potential of harming crops.

The limitations of current robotic weeding solutions such as potential crop damage, environmental concerns, and inefficiency highlight the critical need for more precise methods of targeting and removing weeds to ensure efficient weed management. Laser technology has emerged as a promising alternative. Laser weeding

offers a solution for precise, targeted elimination of weeds, minimizing disruption to the surrounding crop and environment. Treating weeds with lasers has proved effective in eliminating them or stunting their growth (Heisel et al., 2001; Mathiassen et al., 2006; Marx et al., 2012; Kaierle et al., 2013; Mwitta et al., 2022). Narrow beams from lasers can remove both inter-row and intra-row with precision targeting.

The development of autonomous laser weeding robots is still a relatively new endeavor being studied. For example, Xiong et al. (2017) developed a prototype of an autonomous laser weeding robot that utilized color-segmentation for weed identification, fast path-planning algorithms, and two laser pointers to target weeds in an indoor environment, achieving a hit rate of 97%. However, there have been relatively few examples of applications in outdoor field environments.

In this study, we developed and tested an autonomous laser weeding Ackerman-steered robot with a 2-degrees of freedom Cartesian manipulator, stereo vision system, and a diode laser mounted on a pan-and-tilt mechanism. This research builds upon our previous studies, Mwitta et al. (2022), which observed that inexpensive low-powered laser diodes can be used as a weed control mechanism, leading to portable inexpensive robotic platforms, Mwitta et al. (2024) which demonstrated that the deep learning model YOLOv4-tiny can be an ideal solution for real time robotic application due to its speed of detection and satisfactory accuracy in weed detection, and (Mwitta and Rains (2024)) which explored the effectiveness of combining GPS and visual sensors for autonomous navigation in cotton field. This current study leverages the insights from these preceding studies to create a more comprehensive solution for autonomous laser weeding in cotton fields.

This study is driven by the desire to create an affordable, small-scale autonomous robotic platform for farmers. This platform would utilize laser weeding technology for precise and effective weed elimination, minimizing soil disturbance and environmental impact. The potential benefits of this approach are numerous. Autonomous laser weeding offers a more precise and efficient method of weed control compared to traditional methods, potentially reducing herbicide use and promoting sustainable agricultural practices with minimal environmental risks. Furthermore, autonomous robots can alleviate the need for costly manual labor in weed control, leading to increased crop yields by effectively managing weeds and minimizing competition for resources. Compared to mechanical weeding methods, laser weeding minimizes soil disturbance, promoting soil health and structure. An additional benefit is the potential for data-driven weed management. Autonomous systems can collect valuable data on weed location, species, and density, facilitating the development of more targeted weed control strategies. Multiple small robots working together can address larger fields. However, there are challenges to address. Autonomous laser weeding technology is relatively new and requires further development to improve its effectiveness, speed, and reliability under various field conditions. The system's ability to accurately identify and target specific weeds while avoiding damage to crops needs further refinement. A thorough evaluation of laser weeding's potential impact on

beneficial insects and other non-targeted organisms is crucial, as evident in [Andreasen et al. \(2023\)](#). Finally, safety regulations governing the use of high-power lasers in agricultural settings may need to be developed or adapted.

The study contributes to the efforts advancing the field of precision weeding by successfully developing and testing several key components in a real-world setting of a cotton field such as:

- **Agricultural Robotic Platform:** We designed and built a functional robotic platform specifically tailored for agricultural applications.
- **Weed Detection with Deep Learning:** A weed detection mechanism was developed utilizing deep learning technology to accurately identify weeds in the field.
- **Weed Tracking:** The system incorporates a weed tracking mechanism to maintain focus on target weeds as the robot navigates.
- **Autonomous Navigation in Cotton Fields:** A combined visual and GPS-based autonomous navigation system was developed to enable the robot to efficiently navigate within cotton fields.
- **Precision Laser Weeding:** A mechanism for precise weed targeting and elimination using diode lasers was integrated into the platform.

The remaining sections of the article delve deeper into the specifics of this research and its findings. The “Materials and Methods” section provides a detailed account of the development process. It outlines the robotic platform setup, the weed detection mechanism using deep learning, the autonomous navigation system, the real-time weed tracking approach, and the experiments conducted for laser weeding in the cotton field. Following this, the “Results” section presents the key findings and observations from the field experiments. Finally, the “Discussion” section delves into a broader discussion of the developed platform including the strengths and weaknesses identified during testing, potential challenges to consider for future development, and promising avenues for further research.

2 Materials and methods

2.1 The platform setup

The robot (see [Figure 1](#)) used in this study was an electric-powered 4-wheel Ackerman-steered rover with a 2D cartesian manipulator mounted on the front. We developed the robot to navigate between crop rows of 90 cm or more in agricultural fields. The robot had a length of 123 cm and width of 76 cm (without peripherals attached).

The robot had four main controllers (see contextual diagram; [Figure 2](#)) which controlled all the sensors and actuators mounted on the robot: A master controller for coordination of all robot activities, a rover controller for navigation, an arm controller for manipulation, and a laser controller for weed elimination.

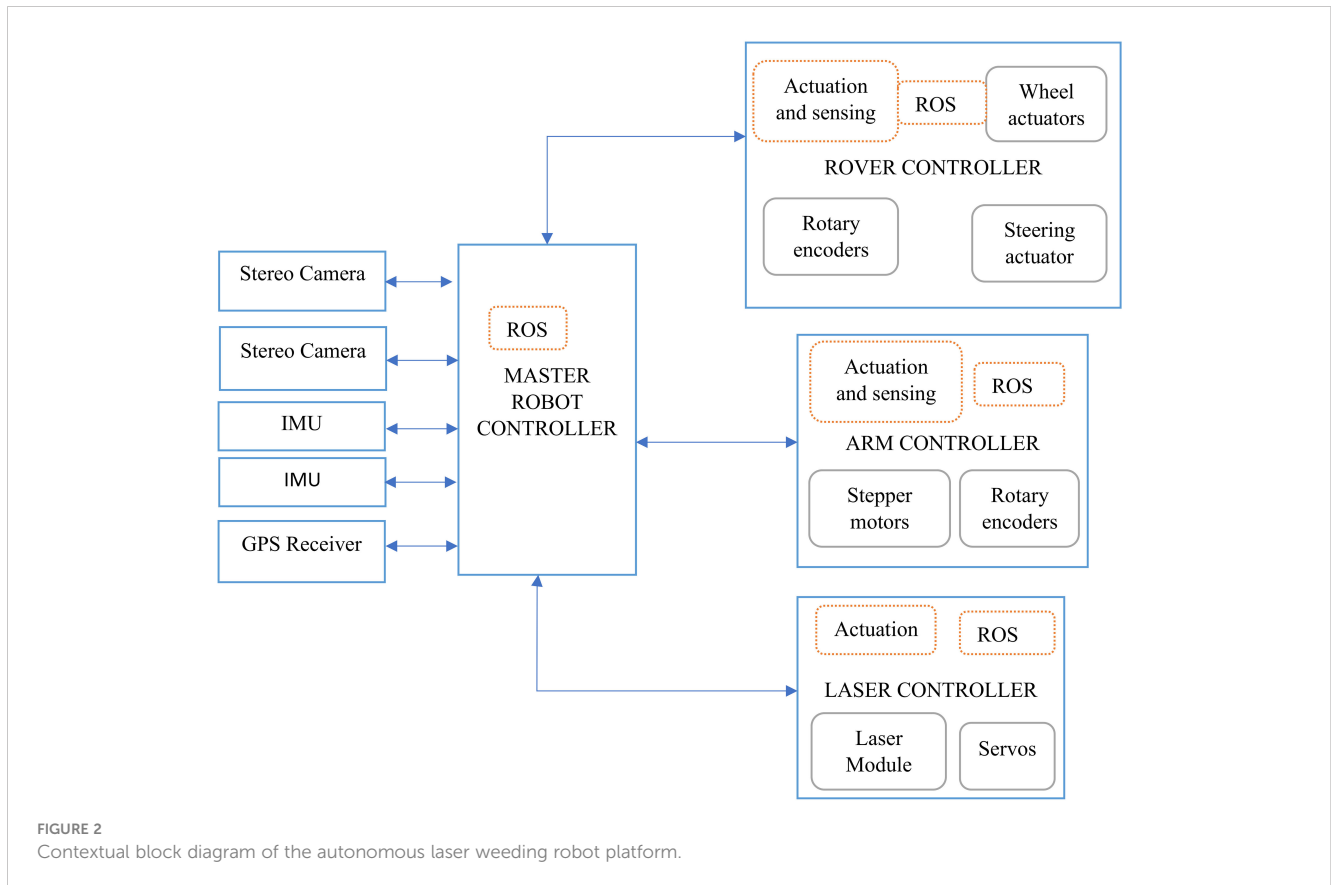
2.1.1 Master robot controller

An embedded computer (Nvidia Jetson Xavier AGX) was used as the central processor of the robot. Equipped with an 8-core ARM v8.2 64-bit CPU, 32GB of RAM, and a 512-core Volta GPU with tensor cores, this embedded computer delivered the needed performance, and enabled creation and deployment of end-to-end AI robotic applications while not demanding a lot of power (under 30W). The computer was responsible for all the autonomous operations, such as receiving and interpreting data from sensors like the stereo cameras, IMUs, and GPS, running deep learning models for weed detection, path planning and navigation between rows, and controlling the Arduino microcontrollers which were directly connected to relays and drivers for sensors and actuators, by sending commands and receive sensors information. The information exchange between the computer and other modules was done using Robotic Operating System ([Quigley et al., 2009](#)) (ROS 1 - Noetic). The computer was powered by a 22000mAh 6-cell Tunigy LIPO battery.

A single-band EMLID Reach RS+ RTK GNSS receiver was mounted on the rover and connected to the embedded computer for robot’s GPS position tracking, field mapping, and navigation. To track the robot’s orientation, two PhidgetSpatial Precision 3/3/3 high resolution inertia measurement units (IMUs) were mounted on the robot. The IMUs contained a 3-axis accelerometer, 3-axis gyroscope, and 3-axis compass for precise estimation of robot’s orientation.



FIGURE 1
The robot platform for laser weeding.



Two stereo cameras (Zed 2 and Zed 2i) from Stereo Labs, were mounted on the robot and connected to the embedded computer. Each of the stereo cameras featured two image sensors that allowed for the capture of normal RGB images, depth images, and 3D point clouds, facilitating 3D pixel depth estimation. Additionally, they were equipped with internal IMUs capable of tracking their orientations.

The platform utilized Zed 2 camera for detecting paths between cotton rows, enabling visual navigation, while the Zed 2i camera was employed for weed detection in the field and the determination of their 3D locations relative to the camera. These cameras published ROS topics for RGB images and point cloud, to which the embedded computer subscribed. To obtain the 3D location of detected weed, the Zed ROS coordinate frames (see Figure 3A) were utilized. The Zed 2i camera publishes a 3D point cloud that contained (x, y, z) values representing the center of the detected weed. Since the camera is mounted at an angle $\theta = 25^\circ$ from the vertical axis (see Figure 3B), the position values published had been rotated on camera's y-axis. To obtain the actual perpendicular distances, the values needed to be rotated back (rotated $-\theta$ degrees by y-axis). The rotation matrix by y is given by:

$$R_y(-\theta) = \begin{bmatrix} \cos(-\theta) & 0 & \sin(-\theta) \\ 0 & 1 & 0 \\ -\sin(-\theta) & 0 & \cos(-\theta) \end{bmatrix}$$

The distances (X, Y, Z) are given by:

$$\begin{bmatrix} X \\ Y \\ Z \end{bmatrix} = R_y(-\theta) \begin{bmatrix} x \\ y \\ z \end{bmatrix}$$

With rover to camera distance (d), camera to end-effector distance (m), and camera to ground height (H), all known, the important distances are calculated as follows:

$$\text{Rover to weed distance} = d + Z$$

$$\text{End effector to weed } (n) = Y - m$$

$$\text{Weed height } (h) = H - X$$

2.1.2 Rover controller

An Arduino Mega microcontroller controlled the driving and steering of the robot. ROS was used to communicate with the embedded computer. Each of the robot wheels was run by a 250W Pride Mobility wheelchair motor with the two back wheels connected to Quadrature rotary encoders (CUI AMT 102), to provide feedback on wheel rotation. The motors were driven by two Cytron MDDS30 motor controllers and powered by two 20000mAh 6-cell Tunigy LIPO batteries. A linear servo (HDA8-

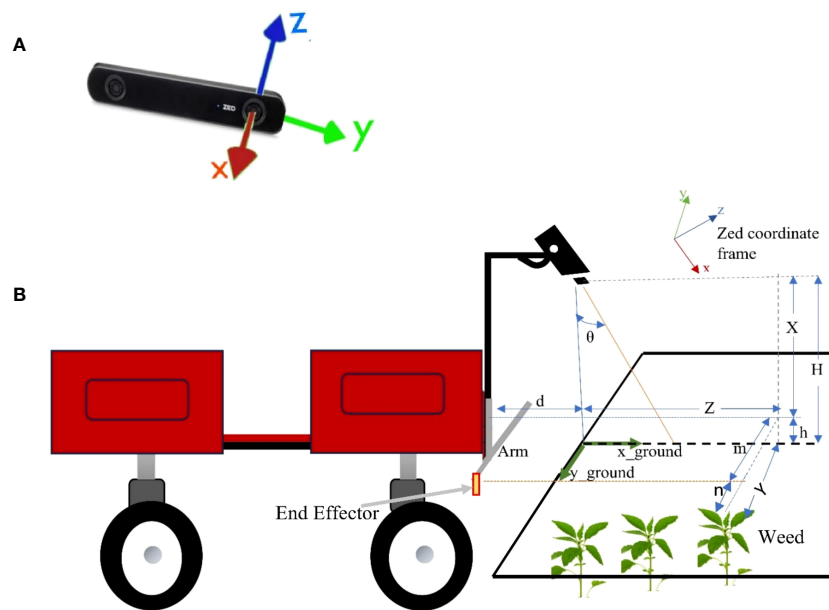


FIGURE 3

(A) Zed camera ROS coordinate frames, (B) Camera setup on the rover. θ is the camera angle from vertical axis, d is rover to camera distance, m is camera to end-effector distance, H is camera to ground distance, and h is height of the weed.

50) was connected to the front wheels for steering. The robot could also be manually controlled using an IRIS+ RC transmitter which communicated with an FrSky X8R receiver connected to the Arduino.

The robot used Ackerman steering geometry (see Figure 4A) to track its position, orientation, and velocity.

With R , the turning radius of the robot, L the wheelbase, W the width of the robot, V the linear velocity of the robot, ∞ the heading, and θ ideal front wheel turning angle, the kinematics of the robot are described as below:

$$\dot{X}_{robot} = V \cos(\infty)$$

$$\dot{Y}_{robot} = V \sin(\infty)$$

$$\dot{\infty} = \frac{V}{L} \tan(\theta)$$

To maintain velocity on uneven agricultural terrain, the robot employed a PID (Proportional, Integral, and Derivative) controller (Ang et al., 2005; Wang, 2020). A PID controller continuously computes the difference between a desired setpoint value and a measured variable, subsequently applying corrections to the control value based on three pre-tuned gains: proportional, integral, and derivative. The PID controller was also used to move the robot to a specific position. For instance, when the position of the detected weed relative to the robot's end-effector was determined, the robot had to move a certain distance to align the end-effector with the weed for elimination. The PID controller made sure the robot didn't overshoot or undershoot the desired position. The feedback (measured value) was obtained from the fused wheel encoders.

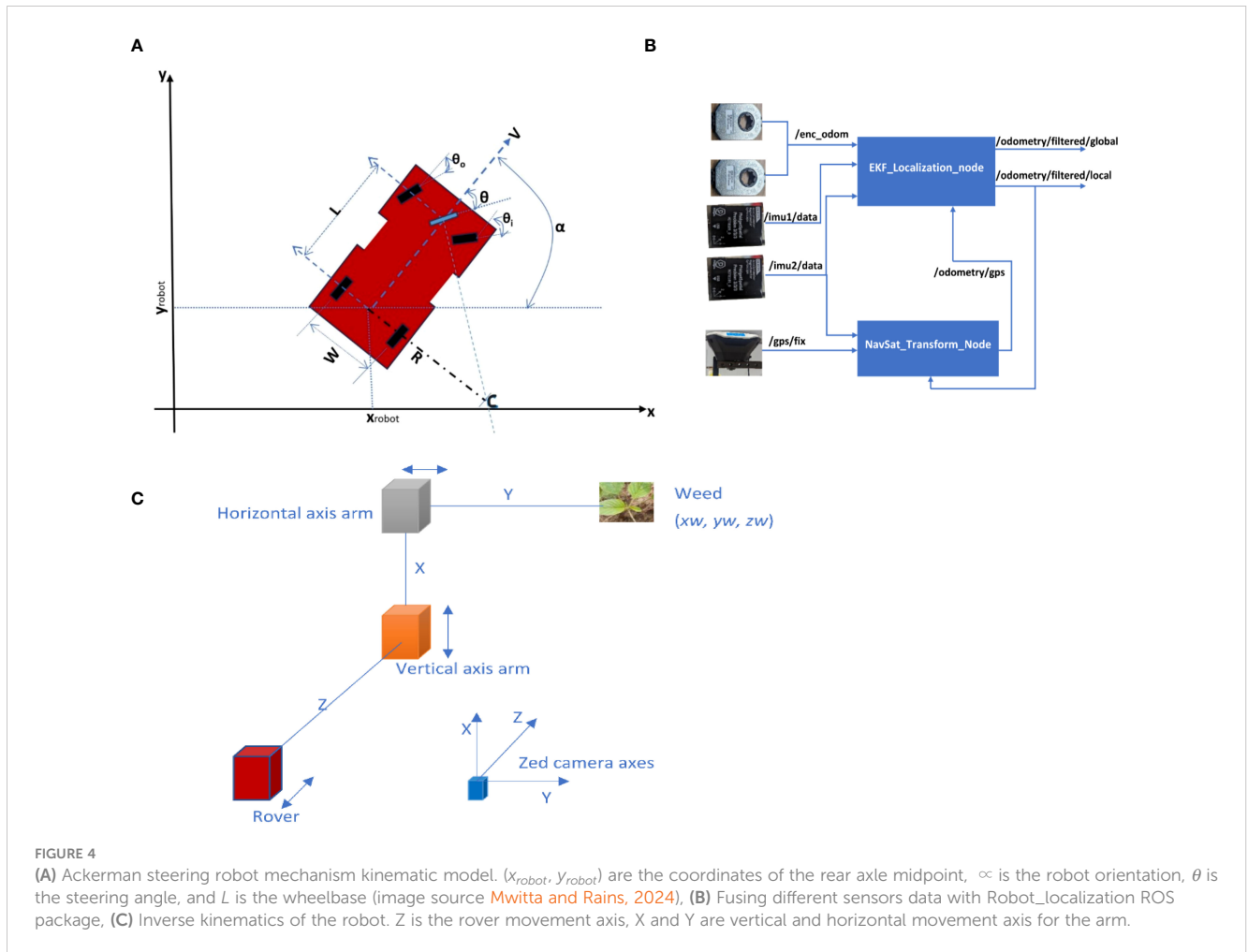
The PID system calculates the motor command required by the robot to reach the desired target, whether it is velocity or position, using three gains: proportional gain K_p , integral gain K_i , and derivative gain K_d . Given the error $e(t)$ as the difference between the current value and the target value, the motor command $u(t)$ was calculated as follows:

$$u(t) = K_p e(t) + K_i \int_0^t e(\tau) d\tau + K_d \frac{de(t)}{dt}$$

The PID controller was tuned to find the values of the three gains (K_p , K_i , K_d) by iteratively adjusting the gains while monitoring the step response of the rover to achieve desired performance.

Due to sensor noise, the accurate estimation of the robot's pose employs an extended Kalman filter (EKF) (Smith et al., 1962). The EKF is designed to fuse multiple noisy sensors by tuning the corresponding sensor variables' noise covariance matrices, resulting in a precise estimate of the robot's pose. The EKF implementation fused continuous data from encoders, IMUs and GPS using the ROS package Robot_localization (Moore and Stouch, 2016). Robot_localization package accepts data including position, linear velocity, angular velocity, linear acceleration, and angular acceleration from sensors, and then estimates robot's pose and velocity. It utilizes two ROS nodes: a state estimation node EKF_localization_node and a sensor processing node NavSat_Transform node (see Figure 4B). These nodes work together to fuse the sensor data and publish an accurate estimate of the robot's pose and velocity.

Using ROS, the rover controller published the position and velocity topics and subscribed to motor command topics from the master controller.



2.1.3 Arm controller

The robotic manipulator was a 2D cartesian system consisting of two Igus drylin[®] belt drive cantilever axis rails (ZAW-1040 horizontally oriented, and ZLW-1040 vertically oriented), driven by two Igus drylin[®] NEMA 17 stepper motors. These motors were controlled by two SureStep STP-DRV-6575 stepper drivers and featured internal rotary encoders to track the position of the rails. The arm was controlled by an Arduino Mega microcontroller which communicated with the embedded computer using ROS. The arm controller published the arm position topic, to which the master controller subscribed. It also subscribed to the arm control topic from the master controller, receiving commands to move to a specific target position.

The manipulator could move left, right, up, and down, with each axis controlled by its respective PID controller. However, the manipulator's movement was constrained by the arm kinematics, allowing translation in two axes only.

For visual servoing, the robot utilized the inverse kinematics of both the arm and rover. Solving the inverse kinematics problem for the robot involved accounting for both the arm movement (X, Y) and the rover movement (Z). Consequently, given the (x_w, y_w, z_w) coordinates of the weed obtained from the stereo camera, the robot had to move a distance of (X, Y, Z) to reach the weed (see [Figure 4C](#)).

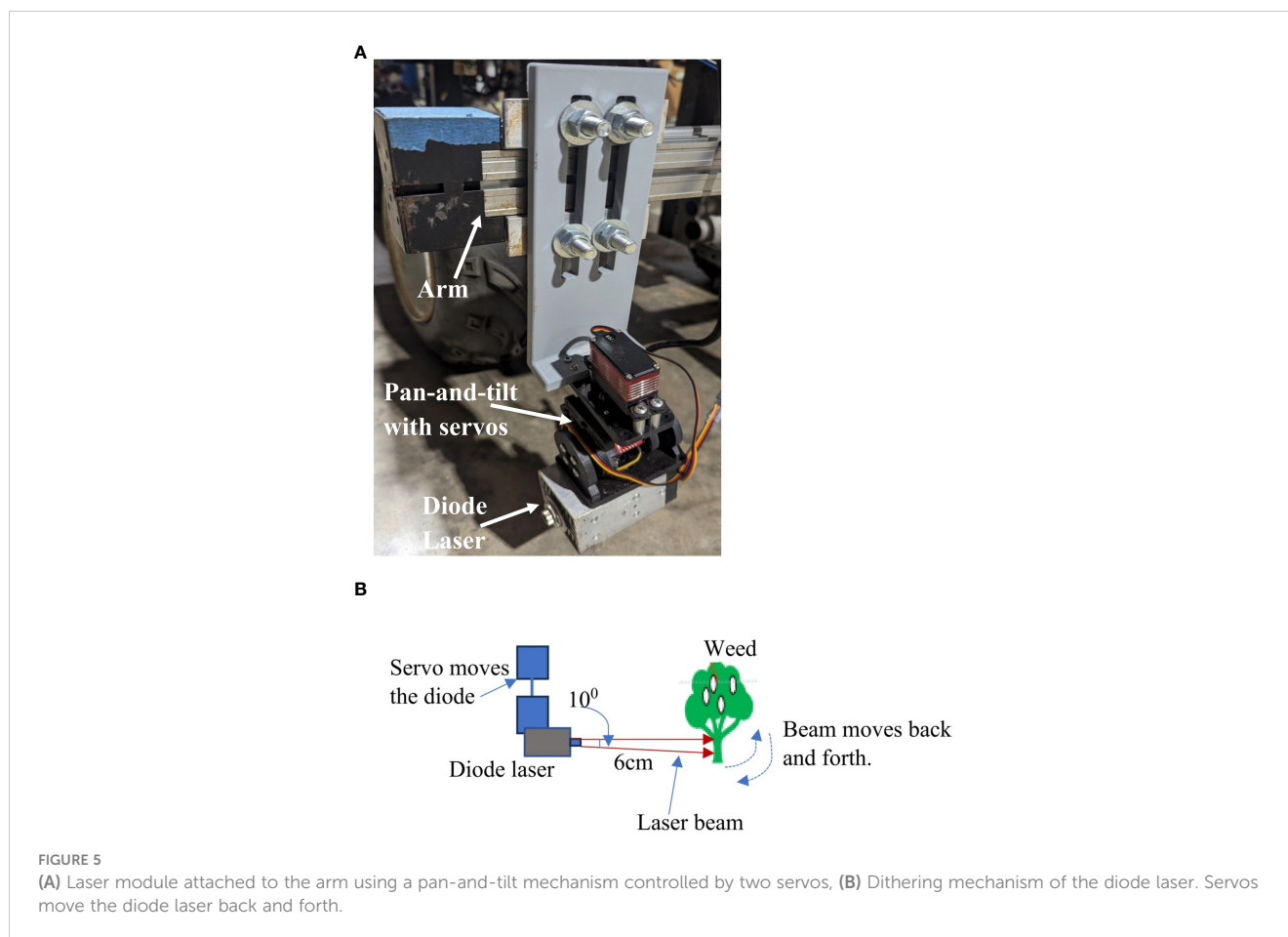
2.1.4 Laser controller

An Arduino Uno was responsible for controlling the release of laser beam from a diode laser. The diode laser was attached to a pan-and-tilt unit, which was controlled by two HSB-9380TH brushless servos, allowing it to rotate to different orientations (see [Figure 5A](#)). The Arduino communicated with the computer through ROS.

Due to the challenge of precisely targeting the weed stem, the servos would dither the diode dither back-and-forth at a speed of 10 times per second at an angle of approximately 10° . This motion increased the cross-section area of the laser beam and maximized the laser beam's contact with the weed stem (see [Figure 5B](#)). The beam formed about 1cm cross-section at the weed stem approximately 3mm above the ground.

2.2 Weed detection using YOLOv4-tiny

We trained YOLOv4-tiny detection model to detect Palmer Amaranth (*Amaranthus palmeri*) weed species in the cotton field. YOLOv4-tiny is a lightweight, compressed version of YOLOv4 ([Bochkovskiy et al., 2020](#)), designed with a simpler network structure and reduced parameters to make it ideal for deployment on mobile and embedded devices. Since the robot was powered by



an embedded computer, a lighter network was necessary to ensure faster inference times. Additionally, performance test on weed detection demonstrated that YOLOv4-tiny was only approximately 4.7% less precise than YOLOv4. However, it offered significantly faster inference, achieving 52 frames per second (fps) on the embedded computer as demonstrated in Mwitta et al. (2024).

Images from the left lens of Zed 2i stereo camera were passed to YOLOv4-tiny model for detecting palmer amaranth weeds. The model performed well in detecting the weeds (see Figure 6A), even when there were shadows (as shown in Figure 6B). However, the model faced challenges in direct sunlight, resulting in excessive reflections and significant shadows (as seen in Figure 6C). This issue was more prevalent during the afternoons one hour after solar zenith and approximately 3 hours before sunset.

2.3 Navigation in cotton fields

To navigate between the rows of cotton, we employed a combination of GPS and visual navigation. We trained a fully convolutional neural network (FCN) for semantic segmentation model (Long et al., 2015) to detect paths between cotton rows in the field. The model achieved a pixel accuracy of 93.5% on the testing

dataset. The detected path between the cotton rows was then mapped from the image domain to the ground plane to obtain the points on the ground that the robot could traverse (see Figure 7A).

GPS was employed as a global planner to map the entire field and acquire pre-recorded coordinates of the path that the robot should follow (as seen in Figure 7B).

We used a local path planner, the Dynamic Window Approach (DWA) (Fox et al., 1997), to navigate between the rows and avoid running over crops based on the path detected by FCN. The DWA algorithm aims to find the optimal collision-free velocities for the robot's navigation, taking the robot's kinematics into account. The ground coordinates of the detected path boundaries were sampled and treated as obstacles in the DWA algorithm (see Figure 7C). While the DWA algorithm proved to be a suitable choice for path planning, it came with the potential drawback of increased computational cost.

In summary, the robot attempted to follow the global GPS map of pre-recorded GPS coordinates while simultaneously avoiding obstacles, represented by the path boundaries from FCN model-detected path, using the DWA algorithm. During field testing, this approach navigated the robot with an average lateral distance error of 12.1 cm between the desired path and the robot's actual path as demonstrated in Mwitta and Rains (2024).



FIGURE 6

(A) Palmer amaranth weed detection in the cotton field, (B) Detecting weeds in presence of shadows during lower sunlight, (C) Sunlight brightness and shadows hindering weed detection.

2.4 Overall robot control with finite state machine

To model the order of task execution and the flow of information between the robot controllers, the master controller (embedded computer) utilized ROS python library SMACH to create a Finite State Machine (FSM). FSM is used to model logic and can be in a specific state from a finite set of possible states at any given point. Furthermore, it can transition to another state by accepting input and producing output.

We modeled the autonomous weeding robot tasks into eight states (actions), with eight transitions from one state to another (see

Figure 8). The states were built in a task-level architecture, allowing the robotic system to transition smoothly from one state to another.

The system begins at the entry state (“get image”), if the system fails to obtain an image from Zed 2i camera, it exits. Otherwise, the weed detection model searches for weeds in the image. If no weed is detected, the system continues navigating between the rows while attempting to acquire another image and run the weed detection program. When a weed is detected, the system obtains the 3D coordinates (x, y, z) of the weed relative to the camera and calculates the forward distance from the rover to the weed, as well as the lateral distance of the weed relative to the laser module attached on the arm. The rover then moves to the weed and orients the arm with

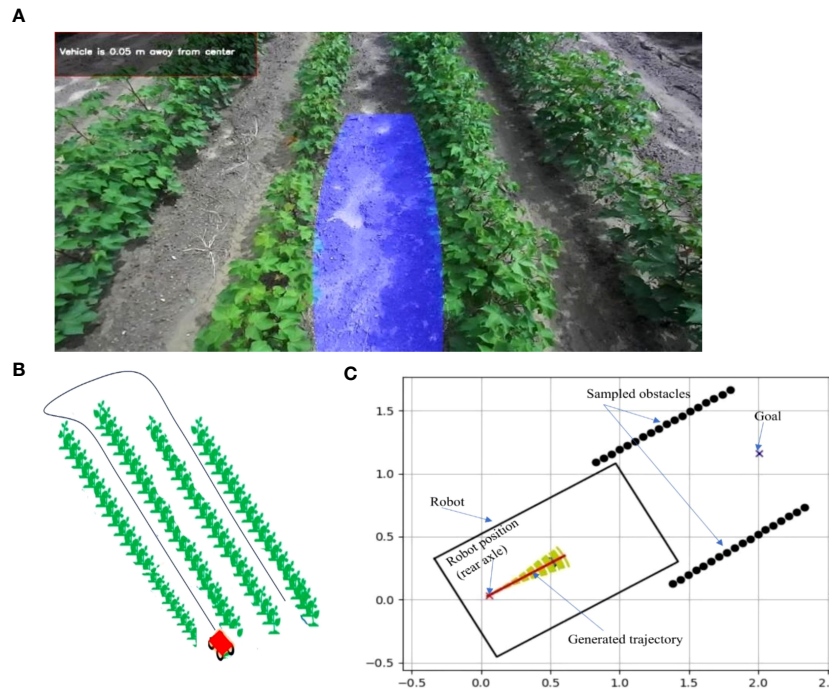


FIGURE 7

(A) Path detected between cotton rows using FCN and mapped to the ground plane, (B) The robot's movement pattern in the field (C) Sampled path boundaries treated as obstacles by the DWA path planning algorithm.

the weed. Subsequently, the arm moves laterally to within 6cm from the weed. At this point, the system emits a laser beam for a defined duration while the servos oscillate to increase the contact area with the weed stem. The arm then returns to its initial position to avoid colliding with cotton in the rows during movement. Then FSM transitions back to the beginning state to start all over.

2.5 Real-time tracking of weeds using DeepSORT algorithm

Relying solely on the PID system to align the robot with the weed position has the drawback of occasional overshooting or

undershooting the desired position. While the dithering of the pan-and-tilt mechanism mitigates part of this problem by increasing the cross-section area of the beam, the unevenness of the agricultural environment can lead the PID system to miss the target by a greater margin than dithering can compensate for. To address this issue, tracking the detected weeds across subsequent frames increases the likelihood of accurately targeting the weed with a laser beam. This is achieved by using the servos on the pan-and-tilt mechanism to point the laser in the direction of the closest weed. Even if the PID system overshoots or undershoots the position, tracking provides the final position of the target relative to the diode's position. The servos then compensate for any error by directing the diode laser towards the targeted weed.

DeepSORT (Wojke et al., 2018), an evolution of the SORT (Simple Online and Realtime Tracking) algorithm (Bewley et al., 2016), enhances object tracking by incorporating a deep learning metric as an appearance descriptor to extract features from images. SORT is a multi-object tracking algorithm that links objects from one frame to another using detections from object detection model, Kalman Filter (Kalman, 1960) for predicting object movements, a data association algorithm [Hungarian algorithm (Kuhn, 1955)] for associating tracks with detected objects, and a distance metric (Mahalanobis distance) for quantifying the association. DeepSORT introduces the appearance feature vector, which accounts for object appearances and offsets some of the Kalman filter's limitations in tracking occluded objects or objects viewed from different viewpoints.

The feature descriptor needs a feature extractor, which is a deep learning model that can classify and match features of the objects

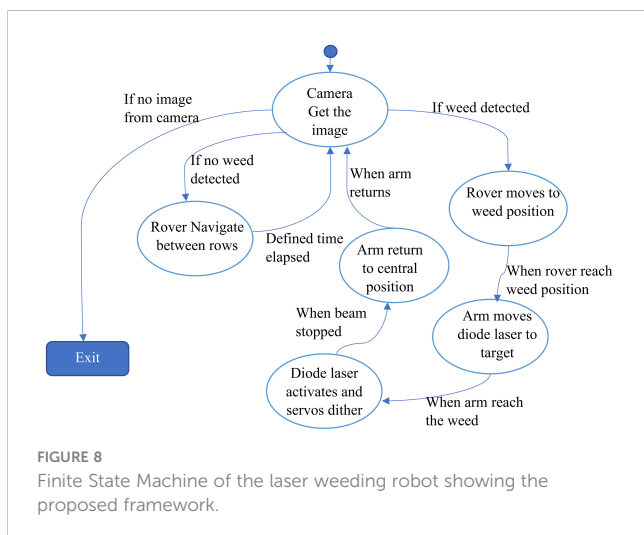


FIGURE 8

Finite State Machine of the laser weeding robot showing the proposed framework.

that are tracked. In this study, a Siamese neural network (Koch et al., 2015) was used as a feature extractor. Siamese networks are renowned for their proficiency in feature matching, by ranking similarities between inputs using a convolutional architecture. We trained the Siamese network model on a dataset of palmer amaranth weed species to learn their features, achieving an accuracy of 89% when evaluated on testing dataset.

DeepSORT performed effectively in conjunction with YOLOv4-tiny as the object detector, assigning ID to every weed detected (see Figure 9A). It attempted to track and maintain the same ID for each weed in subsequent frames. When tested with videos collected by the rover in the field, DeepSORT achieved a Multiple Object Tracking Accuracy (MOTA) of 69.8%. By observing each frame t in a series of frames, with FN representing false negatives, FP representing false positives, IDS denoting ID switches, and GT signifying the ground truth object count, the MOTA is calculated by the following formula:

$$MOTA = 1 - \frac{\sum_t FN_t + FP_t + IDS_t}{\sum_t GT_t}$$

Despite the strong performance of the DeepSORT algorithm, challenges persisted, including issues with ID switching and missed detections in the field. To enhance the performance of the weed detection model and DeepSORT tracking system, the model can benefit from further training with diverse data encompassing a wider range of scenarios. Additionally, fine-tuning the detection and tracking parameters can further improve accuracy.

2.6 Experiments

To evaluate the effectiveness of the autonomous laser weeding robot, we conducted three main experiments at University of

Georgia Tifton campus cotton fields located at (31°28'N 83° 31'W). In the first two experiments, we transplanted around 20 palmer amaranth weeds per plot in five 30-foot plots. For the third experiment, we transplanted around 10 palmer amaranth weeds per plot in five 15-foot plots. This reduction in weed density was due to the experiment being conducted later in the growing season.

The weeds used in the experiments were collected from the University of Georgia research fields near Ty Ty, GA (31°30'N, 83° 39'W) between one to two weeks after emergence. The weeds were transplanted and left for a week to stabilize before treatment. The laser treatments were administered by the robot in 4 plots, while the fifth plot was left as a control. The autonomous rover navigated between the cotton rows, attempting to detect weeds in real-time and treating them with laser beam. After treatments. We observed the weeds for a week after treatments. A 5W 450nm diode laser (measured 5cm from the laser lens using a Gentec Pronto-50-W5 portable laser power meter.) was employed for the treatments. The laser was equipped with a G7 lens and was powered by a 2200mAh LiPo battery and a constant current source of 4A and a voltage of 12V. The robot positioned the laser diode approximately 6cm distance from the weed stem before releasing the beam, which made the beam width of approximately 4mm at the weed stem.

The laser treatment duration was 2 seconds, resulting in a dosage of 10 Joules (2s*5W). This was selected to maximize the weed elimination potential based on the results from our previous study (Mwitta et al., 2022), that showed 100% laser effectiveness at approximately 10 Joules regardless of the diameter of the weed stem (at early stages of growth).

To mitigate safety risks associated with lasers, a low-power 5W diode laser was used, and the beam path was carefully directed only to the targeted area. Furthermore, all personnel working near the

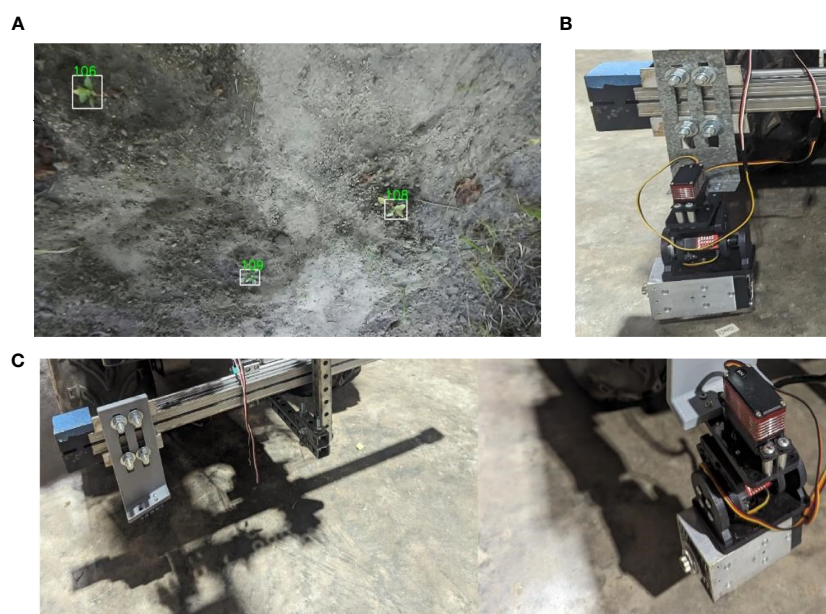


FIGURE 9

(A) ID assigned to detected weeds by the DeepSORT tracking algorithm, (B) Diode laser setup parallel to the ground, (C) The laser module attachment at an angle (10° downwards from horizontal axis), and the laser module attached to it.

robot wore appropriate laser safety glasses with an appropriate rating suitable for the laser being used, and had comprehensive training on laser safety principles and potential hazards. Finally, an emergency stop button readily available to immediately disable the laser in case of unforeseen circumstances was placed on the robot.

2.6.1 First experiment

In the first experiment, the laser module was attached to the arm, positioned parallel to the ground (see Figure 9B). However, due to the distance from bottom of the laser module and the laser mouth, which was approximately 3cm, the laser module needed to be in contact with the ground for the beam to hit the weed stem, unless the weed exceeded a height of about 4cm which was the minimum height for effective targeting. Consequently, during navigation, the arm was raised, and it was lowered when treating the weed to prevent the module from scraping against the ground. The laser treatment duration for each weed was set at 2 seconds. The rover moved at a speed of 0.5 mph, and the robot used a PID controller to reach the target position after detecting the weed.

2.6.2 Second experiment

The second experiment closely resembled the first one, but the laser module was placed at an angle of 10° downward from the horizontal axis (see Figure 9C). This adjustment reduced the arm's up and down movements, thereby increasing the likelihood of targeting even shorter weeds effectively and reducing cycle time between weeds. The laser beam also terminated at the ground, increasing safety from stray laser.

2.6.3 Third experiment

In the third experiment, we implemented DeepSORT algorithm to track the weeds as the robot moved towards the target. The laser configuration remained the same as in the second experiment. Preliminary experiments were conducted in a controlled indoor environment using 15 weeds, to check how tracking influenced the targeting of weeds. Then, the robot was tested in the cotton field.

2.7 Evaluation metrics

We used several metrics to evaluate the effectiveness of the robot in targeting and killing weeds. The accuracy metrics included:

- Total number of detections: All the detections reported by the model.
- True positives: All the detections that were correct.
- False positives: All the detections reported by the model as the targeted weed but were not the targeted weed.
- Laser beam hits: The total number of weeds that the robot attempted to hit and succeeded in hitting them with the laser beam.
- Laser beam misses: The total number of weeds that the robot attempted to hit with the laser beam but missed.
- Hit and killed: The number of weeds which were hit by the laser beam and killed.
- Hit and survived: The number of weeds which were hit by the laser beam but survived after one week on monitoring.
- Percentage killed after hit: The percentage of the weeds killed out of all that were hit by the laser beam.
- Percentage of weeds killed in the plot: The percentage of weeds killed out of all the weeds in the plot.

The speed of operation was measured by the total treatment cycle, which was the total time per single treatment in the worst-case scenario.

3 Results

3.1 Experiment 1

Table 1 shows the results for the first experiment in the field. The biggest challenge was aiming on target (see Figures 10A, B on laser aiming), about 34% of all laser treatments were a miss because of either the weed being shorter than the minimum height (about 38% of the misses), or rover overshooting/undershooting the position due to imperfect sensors (camera, wheel encoders), or a combination of both (The hit rate was 66%). The detection model had a precision of 84%, most of the false positives were due to some other plants in the row looking like palmer amaranth, and the detection misses were due to inconsistencies of illumination in the outside environment, this was minimized by performing the experiments in the morning hours before solar zenith. The laser treatment performed well when the weed was hit, with 87% of the treated weeds killed, but the overall kill rate on a single pass was reduced to 47% due to misses in detection and aiming.

TABLE 1 Treatment results for the first experiment.

Plot No.	Number of weeds	Total number of detections	True Positives	False positives	Laser beam hits	Laser beam misses	Hit and killed	Hit and survived	Percentage Killed after hit (%)	Percentage of weeds killed in the plot (%)
1	21	23	18	5	12	6	10	2	83.33	47.6
2	20	19	16	3	9	5	9	0	100	45
3	23	21	20	1	13	7	10	3	76.92	43.47
4	25	25	20	5	15	5	13	2	86.66	52



FIGURE 10 (A) Laser beam turned on and slightly misses the weed stem due to weed being too short, (B) Top view of laser module targeting a weed.

The robot achieved a total treatment cycle time of 9.5 seconds per weed treatment. The time distribution per task is shown on Table 2. All the weeds in the control plots survived during observation.

3.2 Experiment 2

From Table 3, the detection precision was increased to 91% due to retraining the model with additional images from the first experiment. Only about 19% of detected weeds were missed by the laser with an 81% hit rate. The kill percentage for the treated weeds was about the same (88%), but the overall kill rate on a single pass increased to 63%.

The total treatment cycle time was reduced to 8 seconds due to reduced arm movements with arm moving to target in 2 seconds and arm retracting in 1 second. All the weeds in the control plots survived during observation.

3.3 Experiment 3

The preliminary experiments in a controlled environment achieved a 93% hit rate through tracking, and the servos rotating the diode to point in the direction of the weed (see Figure 11) even when the PID system overshoot/undershot the position.

TABLE 2 Time distribution per task for the first experiment.

Action	Maximum time spent (s)
Weed detection	Real-time
Rover moves to target	3
Arm moves to target	3
Laser treatment	2
Arm retract	1.5
Total treatment cycle	9.5

TABLE 3 Treatment results for second experiment.

Plot No.	Number of weeds	Total number of detections	True Positives	False positives	Laser beam hits	Laser beam miss	Hit and killed	Hit and survived	Percentage Killed after hit	Percentage of weeds killed in the plot
1	23	22	21	1	18	3	16	2	88.88	69.57
2	22	22	19	3	14	5	12	2	85.71	54.54
3	26	24	22	2	17	5	14	3	82.35	53.80
4	19	19	17	2	15	2	14	1	93.33	73.68

In the cotton field, as shown in Table 4, the hit rate was increased through tracking to 83.7%, and the overall kill rate for a single pass was significantly increased to 72.35%. The treatment cycle time remained the same as in experiment 2. All the weeds in the control plots survived during observation.

There were still more than 20% ID switching which proved to be a challenge for the tracking algorithm. In future studies, the model will need to be trained more on the field data obtained from the experiments in addition to tuning of parameters to reduce the ID switching problem.

4 Discussion

In this study, an autonomous diode laser weeding robot was developed and tested in a cotton field. The robot used was an Ackerman-steering ground rover with a 2D cartesian arm that carried a diode laser attached to a pan-and-tilt mechanism to target palmer amaranth weed stems for elimination. Real-time weed detection using YOLOv4-tiny model was employed to detect weeds. The position of the detected weed was determined by the point cloud from Zed 2i stereo camera. The robot used GPS, FCN

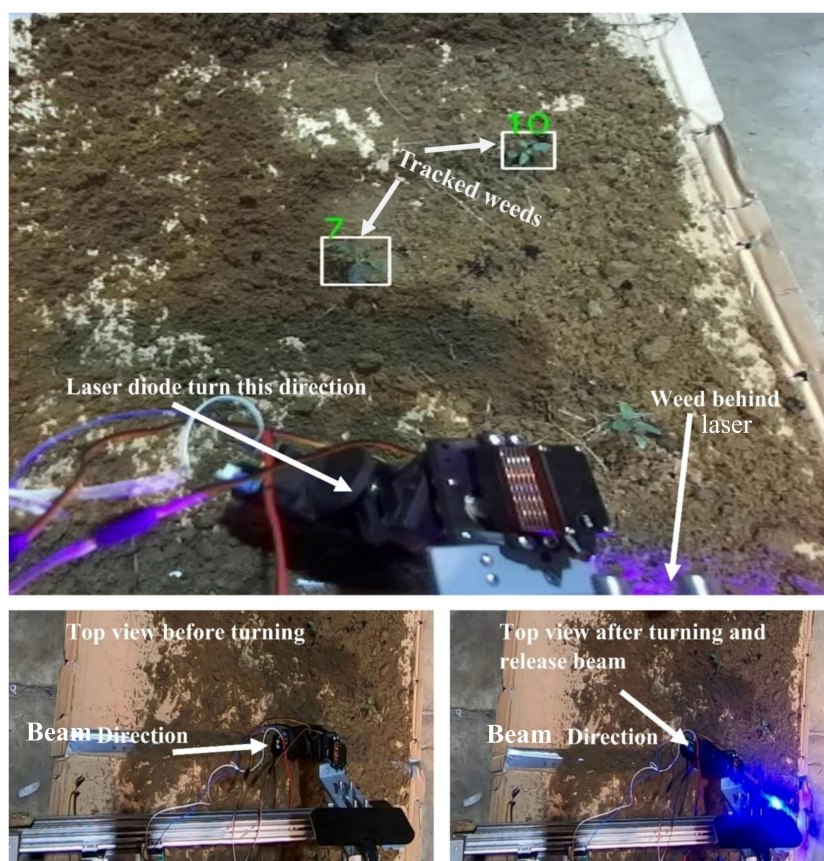


FIGURE 11 Servos rotate the diode laser to compensate the robot overshooting weed position. The direction of diode laser follows the tracked weed.

TABLE 4 Treatment results for third experiment.

Plot No.	Number of weeds	Total number of detections	True Positives	False positives	Laser beam hits	Laser beam miss	Hit and killed	Hit and survived	Percentage Killed after hit	Percentage of weeds killed in the plot
1	11	12	10	1	8	2	8	0	100	72.7
2	9	8	8	0	7	1	6	1	85.71	66.7
3	10	12	10	2	9	1	8	1	88.9	80.0
4	10	13	9	3	7	2	7	0	100	70.0

for semantic segmentation and DWA path planning algorithm to navigate between cotton rows.

Without weed tracking in the field, the robot achieved a hit rate of 66% and 47% overall weed kill rate on a single pass at 9.5 second cycle time per weed treatment when the laser diode was positioned parallel to the ground. A hit rate of 81% with 63% overall kill rate on a single pass at 8 seconds cycle time per weed treatment was achieved when the diode was placed at a 10° downward angle. Using DeepSORT weed tracking algorithm, a preliminary investigation in a controlled environment showed a hit rate of 93%, however, when tested in the field, the robot achieved a hit rate of 83.7% with an overall kill rate of 72.35% at 8 seconds cycle time per weed treatment.

Research into autonomous laser weeding is relatively new; there haven't been many fully implemented solutions. One study similar to ours (Xiong et al., 2017), achieved a 97% hit rate; however, the experiment was conducted indoors in a controlled environment.

The study identified several key challenges that impacted the results, primarily stemming from the inherent complexities of real-world agricultural environments. Factors like sudden changes in illumination, weather variations, shadows, and unforeseen weed emergence significantly affected the robot's ability to detect, track, and navigate visually. While training the deep learning model with more data helped mitigate some of these effects, the system occasionally encountered unexpected scenarios that led to errors. Real-time operation of the robot was hindered by limitations in computational power. This challenge was exacerbated by the simultaneous execution of multiple deep learning algorithms: the detection model, visual navigation system, and DeepSORT weed tracking. The high computational demands of these algorithms resulted in delayed system responses, which in turn contributed to operational errors in the field. Furthermore, the rough terrain of the agricultural field presented difficulties in precisely controlling the rover's velocity and positioning, leading to occasional weed targeting errors. Additionally, the low-powered diode laser used required extended treatment times for effective weed elimination.

Future research will explore several promising avenues for improvement. To enhance the robustness of the deep learning models, we will incorporate a wider range of data encompassing diverse field conditions into the training process. This will allow the models to better handle variations in illumination, weather, and weed appearances encountered in real-world settings. Additionally, exploring the use of 3D point cloud data for path detection and obstacle avoidance holds promise for improved navigation.

By providing a clearer understanding of the environment, 3D perception can lead to more accurate robot movement, especially in challenging terrain. Advanced and adaptable speed control mechanisms, such as Model Predictive Control (MPC), will also be investigated to improve the rover's ability to navigate rough terrain precisely. Finally, optimizing laser weeding efficiency will be a key focus. Investigating strategies like multiple passes of the robot in the field can ensure more effective weed elimination, however, it is crucial to optimize this approach to minimize treatment time and avoid crop damage. Furthermore, as the cost of diode lasers per watt decreases, exploring the use of more powerful lasers can potentially reduce treatment time required for complete weed removal. These future studies hold promise for significantly enhancing the capabilities and overall effectiveness of the autonomous laser weeding platform.

The aim of the study was to develop an affordable system that can be deployed in the field multiple times throughout the season and target weeds at early stages of growth without using chemicals and invasive methods. Despite some minor shortcomings, this platform proves the viability of the concept.

Data availability statement

The raw data supporting the conclusions of this article will be made available by the authors, without undue reservation.

Author contributions

CM: Conceptualization, Data curation, Formal analysis, Investigation, Methodology, Software, Validation, Visualization, Writing – original draft, Writing – review & editing. GR: Conceptualization, Funding acquisition, Project administration, Resources, Supervision, Writing – review & editing. EP: Supervision, Writing – review & editing.

Funding

The author(s) declare financial support was received for the research, authorship, and/or publication of this article. This study was partially funded by US Cotton Incorporated Project 22-727, and US Georgia Peanut Commission.

Acknowledgments

This study is part of a PhD thesis at the University of Georgia titled 'Development of the autonomous diode laser diode' (Mwitta, 2023) which has been made available online via ProQuest.

Conflict of interest

The authors declare that the research was conducted in the absence of any commercial or financial relationships that could be construed as a potential conflict of interest.

References

- Abbas, T., Zahir, Z. A., Naveed, M., and Kremer, R. J. (2018). Limitations of existing weed control practices necessitate development of alternative techniques based on biological approaches. *Adv. Agro.* 147, 239–280. doi: 10.1016/bs.agron.2017.10.005
- Andreasen, C., Vlassi, E., Johannsen, K. S., and Jensen, S. M. (2023). Side-effects of laser weeding: quantifying off-target risks to earthworms (Enchytraeids) and insects (*Tenebrio molitor* and *Adalia bipunctata*). *Front. Agron.* 5. doi: 10.3389/fagro.2023.1198840
- Ang, K. H., Chong, G., and Li, Y. (2005). PID control system analysis, design, and technology. *IEEE Trans. Control Syst. Technol.* 13, 559–576. doi: 10.1109/TCST.2005.847331
- Bastiaans, L., Paolini, R., and Baumann, D. T. (2008). Focus on ecological weed management: What is hindering adoption? *Weed Res.* 48 (6), 481–491. doi: 10.1111/j.1365-3180.2008.00662.x
- Bewley, A., Ge, Z., Ott, L., Ramos, F., and Upcroft, B. (2016). "Simple online and realtime tracking," in 2016 *IEEE international conference on image processing (ICIP)*. (Phoenix, AZ, USA: IEEE), 3464–3468.
- Blasco, J., Aleixos, N., Roger, J. M., Rabatel, G., and Moltó, E. (2002). AE—Automation and emerging technologies: robotic weed control using machine vision. *Biosyst. Eng.* 83 (2), 149–157. doi: 10.1006/bioe.2002.0109
- Bochkovskiy, A., Wang, C.-Y., and Liao, H.-Y. M. (2020). YOLOv4: optimal speed and accuracy of object detection. *arXiv preprint arXiv:2004.10934*. doi: 10.48550/arXiv.2004.10934
- Buhler, D. D., Liebman, M., and Obrycki, J. J. (2000). Theoretical and practical challenges to an IPM approach to weed management. *Weed Sci.* 48 (3), 274–280. doi: 10.1614/0043-1745(2000)048[0274:TAPCTA]2.0.CO;2
- Chauvel, B., Guillemain, J. P., Gasquez, J., and Gauvrit, C. (2012). History of chemical weeding from 1944 to 2011 in France: Changes and evolution of herbicide molecules. *Crop Prot.* 42, 320–326. doi: 10.1016/j.cropro.2012.07.011
- Colbach, N., Kurstjens, D. A. G., Munier-Jolain, N. M., Dalbiès, A., and Doré, T. (2010). Assessing non-chemical weeding strategies through mechanistic modelling of blackgrass (*Alopecurus myosuroides* Huds.) dynamics. *Eur. J. Agron.* 32 (3), 205–218. doi: 10.1016/j.eja.2009.11.005
- Florance Mary, M., and Yogaraman, D. (2021). Neural network based weeding robot for crop and weed discrimination. *J. Phys.: Conf. Series*. (IOP Publishing) 1979 (1), 012027. doi: 10.1088/1742-6596/1979/1/012027
- Fogelberg, F., and Gustavsson, A. M. D. (1999). Mechanical damage to annual weeds and carrots by in-row brush weeding. *Weed Res.* 39 (6), 469–479. doi: 10.1046/j.1365-3180.1999.00163.x
- Fox, D., Burgard, W., and Thrun, S. (1997). The dynamic window approach to collision avoidance. *IEEE Robot Autom. Mag.* 4 (1), 23–33. doi: 10.1109/100.580977
- Gharde, Y., Singh, P. K., Dubey, R. P., and Gupta, P. K. (2018). Assessment of yield and economic losses in agriculture due to weeds in India. *Crop Prot.* 107, 12–18. doi: 10.1016/j.cropro.2018.01.007
- Gianessi, L. P., and Reigner, N. P. (2007). The value of herbicides in U.S. Crop production. *Weed Technol.* 21 (2), 559–566. doi: 10.1614/wt-06-130.1
- Guthman, J. (2017). Paradoxes of the border: labor shortages and farmworker minor agency in reworking California's strawberry fields. *Econ. Geogr.* 93 (1), 24–43. doi: 10.1080/00130095.2016.1180241
- Heisel, T., Schou, J., Christensen, S., and Andreasen, C. (2001). Cutting weeds with a CO₂ laser. *Weed Res.* 41, 19–29. doi: 10.1046/j.1365-3180.2001.00212.x
- Kaierle, S., Marx, C., Rath, T., and Hustedt, M. (2013). Find and irradiate - lasers used for weed control. *Laser Technik J.* 10, 44–47. doi: 10.1002/latj.201390038
- Kalman, R. E. (1960). A new approach to linear filtering and prediction problems. *J. Fluids Engineer. Trans. ASME* 82, 35–45. doi: 10.1115/1.3662552
- Koch, G., Zemel, R., and Salakhutdinov, R. (2015). Siamese neural networks for one shot image learning. *ICML Deep Learn. Workshop*. 2 (1).
- Kuhn, H. W. (1955). The Hungarian method for the assignment problem. *Naval Res. Logist. Q.* 2 (1–2), 83–97. doi: 10.1002/nav.3800020109
- Long, J., Shelhamer, E., and Darrell, T. (2015). "Fully convolutional networks for semantic segmentation," in *Proceedings of the IEEE Computer Society Conference on Computer Vision and Pattern Recognition* (Boston, MA, USA: IEEE), 3431–3440. doi: 10.1109/CVPR.2015.7298965
- Marx, C., Pastrana Pérez, J. C., Hustedt, M., Barcikowski, S., Haferkamp, H., and Rath, T. (2012). Investigations on the absorption and the application of laser radiation for weed control. *Landtechnik* 67, 95–101. doi: 10.15150/lt.2012.277
- Mathiassen, S. K., Bak, T., Christensen, S., and Kudsk, P. (2006). The effect of laser treatment as a weed control method. *Biosyst. Eng.* 95, 497–505. doi: 10.1016/j.biosystemseng.2006.08.010
- McCool, C., Beattie, J., Firn, J., Lehnert, C., Kulk, J., Bawden, O., et al. (2018). Efficacy of mechanical weeding tools: A study into alternative weed management strategies enabled by robotics. *IEEE Robot Autom. Lett.* 3, 1184–1190. doi: 10.1109/LRA.2018.2794619
- Moore, T., and Stouch, D. (2016). A generalized extended Kalman filter implementation for the robot operating system. *Adv. Intell. Syst. Comput.* 302, 335–348. doi: 10.1007/978-3-319-08338-4_25
- Mwitta, C., Rains, G. C., and Prostko, E. (2022). Evaluation of diode laser treatments to manage weeds in row crops. *Agronomy* 12 (11), 2681. doi: 10.3390/agronomy12112681
- Mwitta, C. J. (2023). Development of the autonomous diode laser weeding robot. Georgia, United States: University of Georgia; ProQuest Dissertations and Theses A&I; ProQuest Dissertations and Theses Global. Available at: <https://www.proquest.com/dissertations-theses/development-autonomous-diode-laser-weeding-robot/docview/2917419514/se-2>. (Order No. 30691955).
- Mwitta, C., and Rains, G. C. (2024). The integration of GPS and Visual navigation for autonomous navigation of an Ackerman steering mobile robot in cotton fields. *Front. Robot AI* 11. doi: 10.3389/frobot.2024.1359887
- Mwitta, C., Rains, G. C., and Prostko, E. (2024). Evaluation of inference performance of deep learning models for real-time weed detection in an embedded computer. *Sensors* 24, 514. doi: 10.3390/s24020514
- Oerke, E. C. (2006). Crop losses to pests. *J. Agric. Sci.* 144 (1), 31–43. doi: 10.1017/S0021859605005708
- Oliveira, L. F. P., Moreira, A. P., and Silva, M. F. (2021). Advances in agriculture robotics: A state-of-the-art review and challenges ahead. *Robotics* 10 (2), 52. doi: 10.3390/robotics10020052
- Pérez-Ruiz, M., Slaughter, D. C., Fathallah, F. A., Gliever, C. J., and Miller, B. J. (2014). Co-robotic intra-row weed control system. *Biosyst. Eng.* 126, 45–55. doi: 10.1016/j.biosystemseng.2014.07.009
- Pimentel, D., Lach, L., Zuniga, R., and Morrison, D. (2000). Environmental and economic costs of nonindigenous species in the United States. *Bioscience*. 50 (1), 53–65. doi: 10.1641/0006-3568(2000)050[0053:EAEECON]2.3.CO;2
- Powles, S. B., Preston, C., Bryan, I. B., and Jutsum, A. R. (1996). Herbicide resistance: impact and management. *Adv. Agron.* 58, 57–93. doi: 10.1016/S0065-2113(08)60253-9
- Quigley, M., Conley, K., Gerkey, B., Faust, J., Foote, T., Leibs, J., et al. (2009). ROS: an open-source Robot Operating System. *ICRA workshop Open Source Software*. 3 (3.2), 5.

- Radicetti, E., and Mancinelli, R. (2021). Sustainable weed control in the agroecosystems. *Sustainabil. (Switzerland)* 13 (15), 8639. doi: 10.3390/su13158639
- Richards, T. J. (2018). Immigration reform and farm labor markets. *Am. J. Agric. Econ.* 100 (4), 1050–1071. doi: 10.1093/ajae/aay027
- Schuster, I., Nordmeyer, H., and Rath, T. (2007). Comparison of vision-based and manual weed mapping in sugar beet. *Biosyst. Eng.* 98 (1), 17–25. doi: 10.1016/j.biosystemseng.2007.06.009
- Shaner, D. L. (2014). Lessons learned from the history of herbicide resistance. *Weed Sci.* 62 (2), 427–431. doi: 10.1614/WS-D-13-00109.1
- Smith, G. L., Schmidt, S. F., and McGee, L. A. (1962). Application of statistical filter theory to the optimal estimation of position and velocity on board a circumlunar vehicle. *NASA Tech. Rep.* vol. 135.
- Wang, L. (2020). “Basics of PID Control,” in *PID Control System Design and Automatic Tuning using MATLAB/Simulink*. (West Sussex, UK: John Wiley & Sons Ltd.). doi: 10.1002/9781119469414.ch1
- Wojke, N., Bewley, A., and Paulus, D. (2018). “Simple online and realtime tracking with a deep association metric,” in *Proceedings - International Conference on Image Processing, ICIP* (Beijing, China: IEEE), 3645–3649. doi: 10.1109/ICIP.2017.8296962
- Xiong, Y., Ge, Y., Liang, Y., and Blackmore, S. (2017). Development of a prototype robot and fast path-planning algorithm for static laser weeding. *Comput. Electr. Agric.* 142, 494–503. doi: 10.1016/j.compag.2017.11.023
- Young, S. L., Pierce, F. J., and Nowak, P. (2014). Introduction: Scope of the problem—rising costs and demand for environmental safety for weed control. *Autom.: Future Weed Control Crop. Sys.* 1–8. doi: 10.1007/978-94-007-7512-1_1
- Zahniser, S., Taylor, J. E., Hertz, T., and Charlton, D. (2018). Farm labor markets in the United States and Mexico pose challenges for U. S. Agriculture. *USDA Econ. Res. Ser.* EIB-201. doi: 10.22004/ag.econ.281161